

if the CH stretching (near 2970 cm^{-1}) peak height is chosen as a normalizing factor, the $^1A_2 \rightarrow ^4T_1$ d-d transition is a factor of 2 or 3 weaker in the IETS than in FT-IR. There are also a number of combination bands near 4000 cm^{-1} in the FT-IR spectrum which do not appear in the tunneling spectrum.

Perhaps the most important single feature of this work is the observation of well-defined structure on an electronic transition by tunneling spectroscopy. The spectra presented here very clearly show that shifts and broadening of electronic transitions in IETS are most probably due to chemical interactions between the tunnel junction insulator or top metal and the sample. Tunneling is intrinsically capable of yielding good quality electronic spectra! This will be further emphasized in a future publication concerning the electronic tunneling, FT-IR, and Raman spectra of a series of cobalt complexes.²⁴

A minor but interesting point relates to the very weak band near 5940 cm^{-1} in Figure 2. This is almost certainly an overtone of the 2970 cm^{-1} CH stretch. It is our belief that overtones and combination bands are very very weak in IETS. Even the often quoted Al-O overtone assignment has been severely questioned.²³ Thus the observation of an overtone, even for a strong band such

as the CH stretch, is novel in our experience.

Conclusions

Tunneling spectroscopy is a viable electronic spectroscopy for studying transitions occurring in the IR and near-IR region of the spectrum. Vibronic and/or spin-orbit structuring of electronic transitions may be observed with quality similar to that found in room temperature optical spectroscopy. The selection rules are such that spin- and dipole-forbidden transitions may be observed with significant intensity.

Many of the problems associated with generalizing tunneling to allow the study of low-lying electronic transitions in arbitrary molecular systems have been solved. The remaining major hurdle is posed by the structure of the commonly used tunnel junctions. The production of reliable junctions having less reactive insulators would eliminate the last barrier to complete generalization of IETS to electronic spectroscopy in the IR and near-IR region of the spectrum.

Acknowledgment. We gratefully acknowledge the National Science Foundation and the Division of Materials Research for their support in the form of Grants DMR-8414566 and DMR-8320556. We also thank A. T. Aplin and S. N. Sarkar for their valued assistance.

(24) Hipps, K. W.; Mazur, U., work in progress.

Metalloporphyrin Core Size Resonance Raman Marker Bands Revisited: Implications for the Interpretation of Hemoglobin Photoproduct Raman Frequencies

N. Parthasarathi, C. Hansen, S. Yamaguchi, and T. G. Spiro*

Contribution from the Department of Chemistry, Princeton University, Princeton, New Jersey 08544. Received October 17, 1986

Abstract: Resonance Raman frequencies are examined for high-frequency skeletal modes of several metalloprotoporphyrin derivatives. The previously noted inverse dependence on core size applies to Mn, Co, and Zn as well as to Fe and Ni species, and slightly revised coefficients are derived from the expanded data base. Systematic deviations are noted for 2-methylimidazole adducts of Mn^{II} , Fe^{II} , and Co^{II} and are suggested to be associated with electronic effects of porphyrin doming, or of tilting of the metal-ligand bond relative to the porphyrin plane. Positive deviations are seen for $\text{Cl}_2\text{Sn}^{\text{IV}}$; evidently the correlations break down for so large a central ion ($\text{C}_1\text{-N} = 2.082 \text{ \AA}$). A core-size dependence is also noted for ν_4 , the "oxidation-state marker" for heme proteins, but the slope is much smaller than for the higher frequency skeletal modes, accentuating the negative deviations seen for Fe^{II} , and also Mn^{II} and CO^{II} derivatives; other M^{II} derivatives (Ni, Zn) fall on the line, so there appears to be an electronic basis for the oxidation-state dependence, over and above the core-size dependence. Significantly, the core-size dependence is obeyed for $[(\text{OH})_2\text{Fe}(\text{PP})]^{2-}$, a six-coordinate but high-spin Fe^{II} species. This observation establishes a base line for the core-size analysis of the RR frequencies of the early photolysis product of CO-hemoglobin (Hb) and their shifts relative to deoxyHb. The present results are consistent with the most recent interpretation, that the Fe is out of the heme plane in the photoproduct, but not by as much as in deoxyHb. Core-size correlations are also found for metallo TPP's, but the coefficients differ from those of metallo PP's reflecting the altered normal mode compositions.

Because heme resonance Raman (RR) frequencies show marked sensitivity to redox and ligation state and to the nature of the surrounding protein,¹ there has been strong interest in trying to establish the structural basis of these dependencies via systematic studies of metalloporphyrins. Spaulding et al.² first noted a dependence of one of the high-frequency RR bands on the size of the central cavity in a series of structurally determined metallo octaethylporphyrins, and Huang and Pommier^{3a} found a core-size

dependence for two other bands as well, as did Spiro et al.,^{3b} who analyzed relative effects of core size and doming on these frequencies. In 1982 Choi et al. were able to assign the protoporphyrin (PP) RR spectrum⁴ and to track the modes for a series of Fe derivatives as well as NiPP.⁵ They found that all the skeletal (but not peripheral vinyl) modes above 1450 cm^{-1} showed an inverse linear correlation with core size, and attributed this effect

(1) (a) Spiro, T. G. In *Iron Porphyrins*, Part II; Lever, A. B. P., Gray, H. B., Eds.; Addison-Wesley: Reading, MA, 1983; pp 89-160. (b) Spiro, T. G. *Adv. Protein Chem.* **1985**, *37*, 111-159. (c) Kitagawa, T.; Ozaki, Y. *Struct. Bonding (Berlin)*, in press.

(2) Spaulding, L. D.; Chang, C. C.; Yu, N-T.; Felton, R. H. *J. Am. Chem. Soc.* **1975**, *97*, 2517.

(3) (a) Huang, P. V.; Pommier, J.-C. *C. R. Acad. Sci., Ser. C* **1977**, *285*, 519. (b) Spiro, T. G.; Stong, J. D.; Stein, P. J. *J. Am. Chem. Soc.* **1979**, *101*, 2648.

(4) Choi, S.; Spiro, T. G.; Langry, K. C.; Smith, K. M. *J. Am. Chem. Soc.* **1982**, *104*, 4337.

(5) Choi, S.; Spiro, T. G.; Langry, K. C.; Smith, K. M.; Budd, L. D.; LaMar, G. N. *J. Am. Chem. Soc.* **1982**, *104*, 4345.

to a dependence of the force constant for the methine bridge bonds on the methine angle, the slopes of the correlations varying roughly with the contribution of methine bond stretching to the normal modes.⁵

These correlations became important in interpreting the RR spectra of the transient product of HbCO (Hb = hemoglobin) photolysis, which showed slight but definite downshifts of the core-size marker frequencies⁶ relative to the final product, deoxyHb, those shifts relaxing between 20 and 300 ns after photolysis.⁷ It was suggested⁶ that the expanded core implied by these shifts was due to resistance by the protein to the full out-of-plane displacement of the Fe atom characteristic of deoxyHb. A difficulty with this analysis, however, is that deoxyHb itself deviates somewhat from the core-size correlations as does its model complex (2-MeImH)Fe^{II}PP (2-MeImH = 2-methylimidazole, PP = protoporphyrin), probably because of doming of the porphyrin ring in these five-coordinate out-of-plane hemes.⁵ A desirable reference point would be a planar high-spin Fe^{II} porphyrin. The structure of (THF)₂Fe^{II}TPP⁸ (THF = tetrahydrofuran, TPP = tetraphenylporphine) provides the core size (2.057 Å) for such a complex, but this material, or its PP analogue, has proved to be extremely unstable when exposed as a solid to the Raman laser beam, and it is not clear whether the adduct in THF solution is six- or five-coordinate.

In the present work we report RR spectra for [(OH)₂Fe^{II}PP]₂²⁻ whose composition in solution is unambiguously determined by titration,⁹ and show that it fits the core-size correlations for the expected core size of 2.057 Å. We also reexamine the correlations themselves for a wider range of metallo PP's than were included in the 1982 study,⁵ and revise the coefficients slightly. The first-row transition metals Mn through Zn all obey the correlations, but large positive deviations are seen for Cl₂Sn^{IV}PP, whose extreme core expansion (2.082 Å)¹⁰ appears to put it beyond the range of the correlations. Deviations for some bands are also marked for 2-MeImH adducts of Mn^{II} and Co^{II} as well as Fe^{II} PP's. A common basis for the deviations in these low-valent five-coordinate adducts may involve the electronic effects of porphyrin doming.

A weak core-size dependence has also been uncovered for ν_4 , the C-N porphyrin breathing mode,¹¹ which was identified early as a marker of the Fe oxidation state in heme proteins.¹ The oxidation-state effect lies in negative deviations for Fe^{II}PP's; Mn^{II} and Co^{II} also show negative deviations, but Ni^{II} and Zn^{II} do not. Again specific electronic effects in the low-valent porphyrins are suggested.

Although core-size effects have been noted in RR spectral comparisons of metallo TPP's,^{12,13} they have not previously been studied systematically. We show that the high-frequency skeletal modes all do correlate inversely with core size, although the slopes are different from those seen for PP's, reflecting the different normal mode compositions induced by the altered substituent pattern of the porphyrin peripheral groups. Deviations are also associated with specific chemical effects, as with the PP's. For ClMn^{III}TPP an interesting enhancement is noted for an anomalously polarized ring mode, in resonance with the Soret band, similar to the effect recently noted for (NCS)(MoO)TPP.¹⁴ Mixing of charge transfer and π - π^* transitions via the vibration is the likely source of this enhancement.

Experimental Section

Free-base protoporphyrin IX dimethyl ester (PPDME) and protoporphyrin IX (PP) were purchased from Mid-Century Chemicals (Posen, Ill.) and used without further purification. Cl₂Sn^{IV}PPDME was synthesized from free-base PPDME and stannous chloride as described in ref 15. Mn^{III}PPDME acetate and Mn^{III}PP acetate or chloride were purchased from Mid-Century Chemicals (Posen, Ill.) and used without further purification. The (2-MeImH)Mn^{II}TPP (2-MeImH = 2-methylimidazole) complex was prepared in the same manner as the iron analogue.⁵ A few drops of 0.1 N NaOH solution was added to a few milligrams of ClMn^{III}PP, and this was diluted about three times with distilled water. Excess 2-MeImH (Sigma) purified by resublimation, was added to the solution, followed by the anaerobic addition of a few milligrams of sodium dithionite; a color change to deep red (accompanied by a change in optical absorption from λ 466 and 370 nm (a "split Soret" for the Mn(III) porphyrin) to λ 428 nm for the Mn(II) derivative) indicated complete reduction to give (2-Me-ImH)Mn^{II}PP. The dihydroxy iron(II) protoporphyrin IX complex, [(OH)₂Fe^{II}PP]₂²⁻, was prepared as described by Keilin.⁹ The absorption spectra reported in this reference were reproduced for this species. (2-MeImH)Co^{II}PPDME was prepared by dissolving Co^{II}PPDME complex in degassed toluene (freshly distilled and degassed by the freeze-pump-thaw technique) and adding excess 2-MeImH anaerobically to the solution.

The metallo tetraphenylporphyrins (TPP) were prepared in methylene chloride or toluene. ClFe^{III}TPP, ClMn^{III}TPP, Ni^{II}TPP, Zn^{II}TPP, and Co^{II}TPP were obtained from Mid-Century Chemicals. Sn^{IV}TPP chloride was prepared from free-base TPP [Mid-Century] as described in ref 15. The 2-MeImH adducts of Fe^{II} and Mn^{II}TPP were prepared by adding excess 2-MeImH to a deaerated solution of the ClFe^{III}TPP or ClMn^{III}TPP complex in CH₂Cl₂, followed by anaerobic addition of sodium dithionite-crown ether adduct in CH₃OH. (The latter was prepared by dissolving 12 mg of sodium dithionite (BDH) and 40 mg of 18-crown-6 ether (Sigma) in 1 mL of degassed CH₃OH, and stirring under nitrogen for 15 min.) A color change to deep red indicated complete reduction of the metal from the +3 to the +2 oxidation state.

Resonance Raman spectra were obtained with Ar⁺ (476.5, 514.5 nm), Kr⁺ (406.7, 413.1, 520.8, 530.9, 568.2 nm), and He-Cd (441.6 nm) laser excitation. The samples were spun in an NMR tube positioned in back-scattering geometry, and spectra were obtained with a Spex 1401 double monochromator equipped with a cooled photomultiplier and photon-counting electronics. The data were collected digitally with a MINC (DEC) computer. Spectral slit widths were 5 cm⁻¹, and the laser power at the source was between 50 and 100 mW.

Results and Discussion

A. Spectral Assignments. Choi et al.⁴ assigned porphyrin skeletal and peripheral vinyl modes of NiPP (PP = protoporphyrin IX) via a study of the effects of vinyl deuteration upon the resonance Raman and infrared spectra. (In the ensuing discussion, no distinction is made between protoporphyrin IX or its dimethyl ester, used for aqueous and nonaqueous solutions, respectively. Comparisons of the two for the same metal and ligand set show no significant difference in the porphyrin skeletal frequencies.) The RR bands of a series of iron protoporphyrin derivatives could then be correlated to the NiPP spectrum, and it was found that porphyrin skeletal mode frequencies above 1450 cm⁻¹ all correlated inversely with the porphyrin core size as obtained from crystal structure data.⁵ Since then RR data have been reported for Zn^{II}PP¹⁶ and for the bispiperidine complex of Ni^{II}PP.¹⁷ In this study we extend the data base to PP adducts of Mn^{II}, Mn^{III}, Co^{II}, and Sn^{IV}.

The problem of assigning the bands is not a trivial one because of the large number of modes that are Raman-active for PP.⁴ The intensity pattern is reasonably consistent among the different metalloprotoporphyrins, however, and variable wavelength excitation is very useful. When RR spectra are excited in resonance with the Q absorption bands (~500–600 nm), modes are selectively enhanced which correlate with nontotally symmetric vibrations in the idealized D_{4h} symmetry of the porphyrin ring: A_{2g}, B_{1g}, and B_{2g}.¹ Of particular interest for the present study is the dominance of modes ν_{10} (B_{1g}), ν_{11} (B_{1g}), and ν_{19} (A_{2g}) in the high-frequency region, 1450–1650 cm⁻¹; ν_{28} (B_{2g}) may also appear

(6) (a) Terner, J.; Spiro, T. G.; Nagumo, M.; Nicol, M. S.; El-Sayed, M. A. *J. Am. Chem. Soc.* **1980**, *102*, 3238. (b) Terner, J.; Stong, J. D.; Spiro, T. G.; Nagumo, M.; Nicol, M. S.; and El-Sayed, M. A. *Proc. Natl. Acad. Sci. U.S.A.* **1981**, *78*, 1313–1317. (c) Dasgupta, S.; Spiro, T. G. *Biochemistry* **1986**, *25*, 5941–5948.

(7) Stein, P.; Terner, J.; Spiro, T. G. *J. Phys. Chem.* **1982**, *86*, 168.

(8) Reed, C. A.; Mashiko, T.; Scheidt, W. R.; Spartalian, K.; Lang, G. J. *J. Am. Chem. Soc.* **1980**, *102*, 2302–2306.

(9) Keilin, J. *Biochemistry* **1945**, *45*, 448.

(10) Cullen, D. L.; Meyer, E. F., Jr. *Acta Crystallogr., Sect. B* **1973**, *29*, 2507.

(11) Abe, M.; Kitagawa, T.; Kyogoku, Y. *J. Chem. Phys.* **1978**, *69*, 4516.

(12) Stong, J. D.; Kubaska, R. J.; Shupack, S. I.; Spiro, T. G. *J. Raman Spectrosc.* **1980**, *9*, 312–314.

(13) Chottard, G.; Baccioni, P.; Baccioni, J.-P.; Lange, M.; Mansuy, D. *Inorg. Chem.* **1981**, *20*, 1718–1722.

(14) Terner, J.; Topich, J. *Chem. Phys. Lett.* **1984**, *106*, 508–511.

(15) Fuhrhop, J. H.; Smith, K. M. In *Laboratory Methods in Porphyrin and Metalloporphyrin Research* Elsevier: New York, 1975; p 41.

(16) Feitelson, J.; Spiro, T. G. *Inorg. Chem.* **1986**, *25*, 861.

(17) Kim, D.; Su, O.-Y.; Spiro, T. G. *Inorg. Chem.* **1986**, *25*, 3988.

Table I. Selected Skeletal Mode Frequencies (cm⁻¹) for Metallo Protoporphyrins

complex	C ₁ N ₄ ^a Å	ν_4^o A _{1g}	ν_{28} B _{2g}	ν_3 A _{1g}	ν_{38} E _u	ν_{11} B _{1g}	ν_{19} A _{2g}	ν_2 A _{1g}	ν_{37} E _u	ν_{10} B _{1g}	ref
(Cl) ₂ Sn ^{IV}	2.082 ^b	1377	(1444) ^p	1471	(1509)	1548		1568		1605	this work
(2-MeImH)Mn ^{II}	2.065 ^c	1357		1463	1512	1535	1537	1568		1595	this work
(OH) ₂ Fe ^{II}	2.057 ^d	1355		1469	1522	(1541)		1559	(1579)	(1605)	this work
(DMSO) ₂ Fe ^{III}	2.045 ^e	1370	1447	1480	1518	1545	1560	1559	1580	1610	5
(2-MeImH)Fe ^{II}	2.044 ^f	1357		1471	1521	1547	1550	1562	1583	1604	5
(Pip) ₂ Ni ^{II}	2.038 ^g	1368		1480	1531	1552		1566	1583	1604	17
Zn ^{II}	2.036 ^h	1369		1484	1527	(1550)		1568	1587		16
(Cl)Fe ^{III}	2.019 ⁱ	1373	1453	1491	1533	1553	1571	1570	1591	1626	5
(ImH) ₂ Fe ^{II}	2.004 ^j	1359	1461	1493	1560	1539	1583	1584	1604	1617	5
(Ac)Mn ^{III}	1.990 ^k	1370		1500		1559	1580	1580		1634	this work
(ImH) ₂ Fe ^{III}	1.989 ^l	1373	1469	1502	1554	1562	1586	1579	1602	1640	5
(2-MeImH)Co ^{II}	1.973 ^m	1371		1503	(1553)	1560	1572	1587	1612	1634	this work
Ni ^{II}	1.958 ⁿ	1381	1483	1519	1566	1575	1602	1593	1609	1655	4

^a Core sizes inferred from the following structure determinations: ^b (Cl)₂SnOEP, ref 10. ^c (1-MeIm)Mn^{II}TPP, ref 49. ^d (THF)₂Fe^{II}TPP, ref 8. ^e [(TMSO)₂Fe^{III}TPP]ClO₄, ref 50. ^f (2-MeImH)Fe^{II}TPP, ref 20. ^g (ImH)₂Ni(tetrakis-*N*-methylpyridinium)porphine, ref 51. ^h ZnTPP, ref 52. ⁱ (Cl)Fe^{III}PP. This is the average C₁-N distance for five-coordinate high-spin Fe^{III} complexes given by Hoard, ref 53. ^j (pip)₂Fe^{II}PP, ref 54. ^k (Cl)Mn^{III}TPP, ref 19. ^l [(ImH)₂Fe^{III}TPP]Cl, ref 55. ^m (1-MeIm)Co^{II}TPP, ref 56. ⁿ NiOEP (D_{4h}), ref 2. ^o Mode numbering from ref 11 and 4. ^p Frequencies in parentheses refer to poorly resolved bands. ^q Spectra in this study obtained with excitation at 406.7, ^{g,h} 413.1, ^r 476.5, ^s 520.8, ^t 530.9, ^u and 568.2 nm.¹

Table II. Selected Skeletal Mode Frequencies (cm⁻¹) for Metallo Tetraphenylporphyrins^q

complex	C ₁ N ₄ ^a Å	ν_4^b A _{1g}	ν_{13} B _{1g}	ν_3 A _{1g}	ν_{28} B _{2g}	ν_{12} B _{1g}	ν_{20} A _{2g}	ν_2 A _{1g}	ν_{11} B _{1g}	ref
(Cl) ₂ Sn ^{IV} TPP	2.098	1365		1440	1460	1488		1542		this work
(2MeImH)Mn ^{II} TPP	2.065	1340	1356	1432		1484		1532	1559	this work
(DMSO) ₂ Fe ^{III} TPP	2.045	1356	1361	1438	1451	1486		1541	1547	this work
(2MeImH)Fe ^{II} TPP	2.044	1341	1358	1431	1449			1538		this work
[Fe ^{III} (TPP) ₂]O	2.019	1359		1450		1495	1511	1553	1561	43
(ImH) ₂ Fe ^{II} (TPP)	1.997	1354	1364	1448	1472	1497		1557	1545	this work
Mn ^{III} (TPP)Cl	1.990	1363	1371	1456		1496	1529	1557	1579	this work
(ImH) ₂ Fe ^{III} (TPP)Cl	1.989	1365	1371	1459	1476	1501	1533	1561	1581	this work
(2MeImH)Co ^{II} (TPP)	1.973	1363				1498		1563	1590	this work
Ni ^{II} TPP	1.958	1372		1472		1508	1546	1571		this work

^a Core size from same reference structures as for protoporphyrins (Table I) except (Cl)₂Sn^{IV}TPP. Mode numbering from ref 43.

but is generally weak.⁵ The ν_{11} and ν_{19} bands sometimes overlap, and polarization measurements are needed to make the assignments; ν_{19} is anomalously polarized whereas ν_{11} is depolarized. The actual polarization ratios deviate somewhat from the ideal values because the symmetry of protoporphyrin is lower than D_{4h}, but the polarization rules still apply qualitatively.⁵ With excitation in resonance with the B absorption band (~400 nm), totally symmetric modes (A_{1g}) are enhanced.¹ The ν_4 (C-N breathing)¹¹ mode at ~1370 cm⁻¹ dominates the spectrum, while ν_2 is the strongest band in the 1500–1600-cm⁻¹ region. The third high-frequency A_{1g} mode, ν_3 near 1500 cm⁻¹, is only moderately strong, but is generally well isolated from other bands. On the other hand, ν_2 is flanked by two E_u (infrared) modes, ν_{37} and ν_{38} , which are weakly activated in the RR spectrum by virtue of the asymmetric disposition of the vinyl groups;⁴ these bands are seen only with B-band excitation. The B_{1g} modes ν_{10} and ν_{11} can frequently be detected in B-band excited spectra, probably because of Jahn-Teller activity.¹⁸

These spectral features and their assignments are illustrated in Figure 1 for the case of (2-MeImH)CoPP. Band frequencies for the other derivatives explored in this study are listed in Table I. For Sn^{IV} porphyrins and [(OH)₂Fe^{II}PP]⁻, Q-band excited spectra were unobtainable owing to interference from fluorescence. In these cases ν_{19} frequencies are unavailable, and there may be some uncertainty about the assignment of ν_{11} vs. ν_{38} .

B. Core-Size Correlations and Deviations. Figure 2 shows a plot of skeletal mode frequencies against the porphyrin core size (C₁-N, the porphyrin center to pyrrole N distance) as determined from X-ray crystal structure data. The closed symbols represent bands for which polarizations have been determined, which serve to classify the symmetry species of the vibration¹ (A_{1g}, polarized; A_{2g}, anomalously polarized; B_{1g}, B_{2g}, depolarized). Polarizations

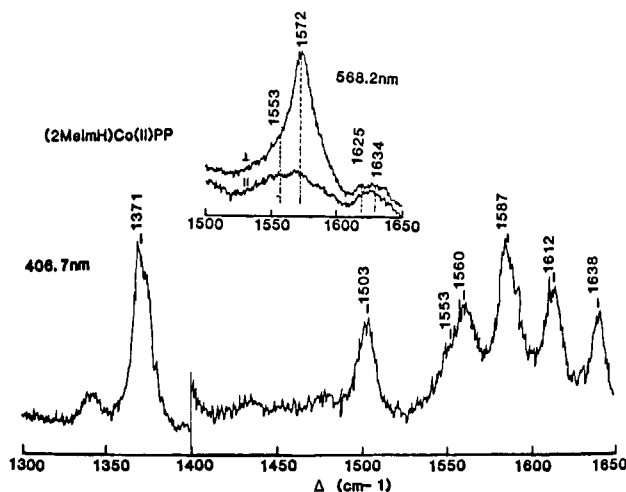


Figure 1. Raman spectrum of (2-MeImH)Co^{II}PPDME (~5 mM) in toluene, excited at 406.7 nm, near resonance with the B absorption band (404 nm). The inset shows a fragment of the spectrum, in parallel and perpendicular polarization, with 568.2 nm near resonance with the Q (555 nm) absorption band. This wavelength emphasizes the anomalously polarized mode ν_{19} , at 1572 cm⁻¹.

are not available for the bands represented by the open symbols, but the frequencies fall close enough to the correlations to indicate the probable assignment. Structures are not generally available for protoporphyrin per se, but Hoard¹⁹ has shown that structure parameters are not significantly dependent on the peripheral substituents for a given central metal and axial ligand set. The actual structures from which the core sizes were obtained are cited

(18) Cheung, L. D.; Yu, N.-T.; Felton, R. H. *Chem. Phys. Lett.* **1978**, *55*, 527.

(19) Hoard, J. L. In *Porphyrins and Metalloporphyrins*; Smith, K. M., Ed.; American Elsevier: New York, 1975; pp 317–376.

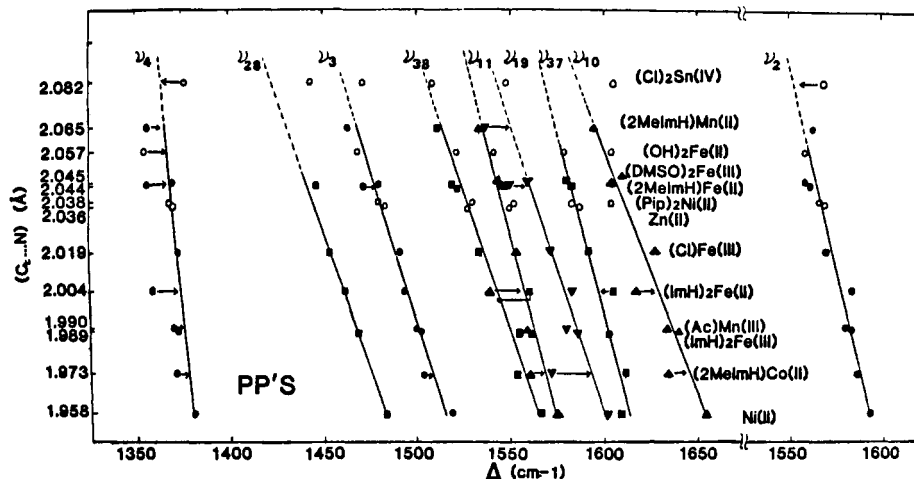


Figure 2. Core size vs. skeletal mode frequencies plotted for the indicated metalloprotoporphyrin complexes. Core sizes are estimated from reference structures cited in Table I. Note the displacement of the frequency scales. Symbols indicate observed polarizations: ●, polarized (A_{1g}); ■, polarized (E_g); ▲, depolarized (B_{1g} , B_{2g}); ▼, anomalously polarized (A_{2g}); ○, polarization undetermined.

Table III. Core-Size Slopes and Intercepts for PP and TPP Skeletal Modes

PP				TPP			
mode ^a	character ^b	K^c ($\text{cm}^{-1}/\text{\AA}$)	A (\AA) ^c	mode ^a	character ^d	K^c ($\text{cm}^{-1}/\text{\AA}$)	A (\AA) ^c
ν_4	CaN	136.7	12.07	ν_4	CaN	138.9	11.81
ν_{37}	C_bC_b	376.7	6.24	ν_{13}	CaN	154.3	10.87
ν_{11}	C_bC_b	353.1	6.42	ν_{12}	C_bC_b	173.6	10.61
ν_2	C_bC_b	329.6	6.78	ν_2	C_bC_b	312.5	6.98
ν_3	C_aC_m	423.7	5.53	ν_3	C_aC_b	347.2	6.19
ν_{19}	C_aC_m	452.0	5.5	ν_{20}	C_aC_m	568.2	4.68
ν_{28}	C_aC_m	494.4	4.96	ν_{28}	C_aC_b	456.4	5.22
ν_{10}	C_aC_m	564.9	4.89	ν_{11}	C_aC_m	555.6	4.83
ν_{38}	C_aC_m	459.0	5.36				

^a PP and TPP mode numberings from ref 11 and 43, respectively. ^b Principal bond-stretching contributor, according to the normal mode calculation of Abe et al.¹¹ ^c Slope and intercept for the best straight line obeying $\bar{\nu} = K(A - d)$ when $d = C_i-N$ (\AA). ^d Qualitative assignments from ref 42 and 43.

in Table I. The correlations are similar to those obtained by Choi et al.,⁵ but now extend to a larger number of species, including representatives from the first-row transition metals Mn, Co, Ni, and Zn, as well as Fe. The slopes and intercepts of the best straight lines ($\bar{\nu} = K(A - d)$, where $d = C_i-N$) are altered slightly (Table III) from those given by Choi et al.⁵

The general consistency of these correlations is remarkably good, although certain complexes show significant deviations. The most dramatic of these deviations, already noted and analyzed by Choi et al.,⁵ are the up- and downshifts for $(\text{ImH})_2\text{Fe}^{\text{II}}\text{PP}$, which are due to back-bonding from low-spin Fe^{II} to the porphyrin π^* (e_g) orbitals (in the absence of strong π acid axial ligands); the signs of the shifts are associated with the symmetry properties of the normal modes and the nodal pattern of the e_g orbitals. Choi et al.⁵ also noted deviations for $(2\text{-MeImH})\text{Fe}^{\text{II}}\text{PP}$ and suggested that they may be due to doming of the porphyrin, seen in the crystal structure of $(2\text{-MeImH})\text{Fe}^{\text{II}}\text{TPP}$,²⁰ and also deoxyMb²¹ and deoxyHb.²² The doming, occasioned by the tilting of the pyrrole rings as they follow the Fe atom out of the plane in the high-spin five-coordinate Fe^{II} complexes, might be expected to disrupt the π conjugation in the porphyrin ring, producing deviations from the core-size lines analogous (although differing in the modes principally affected) to those observed for $(\text{ImH})_2\text{Fe}^{\text{II}}\text{PP}$.

In Figure 2 we see that similar deviations are shown by 2-MeImH adducts of Co^{II} and also $\text{Mn}^{\text{II}}\text{PP}$'s. Low-frequency deviations are especially marked for ν_{19} for all three 2-MeImH derivatives. It is possible that doming provides a common mechanism for the deviations. All three complexes involve

five-coordinate low-valent transition metal ions. The low valence extends the metal d orbitals and accentuates their electronic influence, including the directionality of the pyrrole-metal interaction which favors doming. Other stereoelectronic mechanisms can also be considered. For example, Champion and co-workers²³ have recently called attention to the possibility that tilting of the imidazole ligand in deoxyMb and deoxyHb, seen in their crystal structures, can lower the Fe-imidazole stretching frequency owing to an antibonding interaction of the half-filled d_{z^2} orbital (which is off axis in the tilted complexes) with the filled porphyrin π orbitals. It is conceivable that the high-frequency skeletal modes could also be influenced by this interaction which might apply to the 2-MeImH complexes because of the asymmetric nature of the imidazole ligand.

The core-size plots break down for $\text{Cl}_2\text{Sn}^{\text{IV}}\text{PP}$, which was chosen because of the very large Sn^{IV} core size, 2.082 \AA ¹⁰ (for the OEP analogue). All of the points fall significantly above the extrapolated straight lines; deviations are especially notable for ν_2 and ν_{10} . It seems likely that the electronic effects of expanding the porphyrin core saturate at some point. This point may already be reached at the complex $(2\text{-MeImH})\text{Mn}^{\text{II}}\text{PP}$ ($C_i-N = 2.065$ \AA) which also shows a large positive deviation for ν_2 , as well as the previously noted negative deviations that are in common with the other 2-MeImH complexes. We note that the skeletal frequencies of $(\text{py})_2\text{Ru}^{\text{II}}\text{OEP}$ have recently been shown^{24a} to be in good agreement with the core size, 2.047 \AA .^{24b} (Octaethylporphyrins give skeletal frequencies that are close to those of PP's, except for ν_2 which interacts with vinyl $\text{C}=\text{C}$ stretching in PP's.) Thus, the core-size correlations extend to other than first transition

(20) Hoard, J. L.; Scheidt, W. R. *Proc. Natl. Acad. Sci. U.S.A.* **1973**, *70*, 3919; **1974**, *71*, 1578.

(21) Takano, T. *J. Mol. Biol.* **1977**, *110*, 569.

(22) Fermi, G.; Perutz, M. F.; Shaanan, B.; Fourme, R. *J. Mol. Biol.* **1984**, *175*, 159.

(23) Bangcharoenpaupong, O.; Schomacker, K. T.; Champion, P. M. *J. Am. Chem. Soc.* **1984**, *106*, 5688-5698.

(24) (a) Kim, D. H.; Spiro, T. G. *Inorg. Chem.* **1986**, *25*, 3993. (b) Hopf, F. R.; O'Brien, T. P.; Scheidt, W. R.; Whitten, D. G. *J. Am. Chem. Soc.* **1975**, *97*, 277.

ion metals, and the Sn^{IV} deviations are not ascribable simply to Sn being a third transition row metal.

Figure 2 also contains a core-size plot for ν_4 , a band which has previously been associated with the oxidation state of iron porphyrins,^{1,25,26} and/or with the effects of electron donation into the π^* (e_g) orbital.²⁶⁻²⁹ An underlying core size dependence is also evident for this band, although the slope is appreciably smaller than for the other high-frequency skeletal modes, reflecting a more modest contribution from the methine bonds; pyrrole C-N stretching is the main contributor to this mode.¹¹ The oxidation-state dependence is seen as negative deviations for the Fe^{II} complexes. (2-MeImH)Mn^{II}PP also deviates by about the same amount, while the Mn^{III} representative (acetate complex) falls close to the line as do the Fe^{III} complexes.³⁰ (2-MeImH)Co^{II}PP shows a small negative deviation, while the points for Ni^{II} and Zn^{II} fall on the line. Thus there is evidently a specific electronic effect associated with the low-valent Fe, Mn, and Co species. The role of back-bonding in depressing the ν_4 frequency in low-spin Fe^{II} complexes has long been recognized.²⁶⁻²⁸ Back-bonding is not expected to be important, however, for the high-spin Fe^{II} and Mn^{II} complexes with their long M-N (pyrrole) bonds, and indeed these complexes do not show the same deviations from the core-size correlations discussed above for (ImH)₂Fe^{II}PP. It may be that the highly polarizable high-spin Fe^{II} and Mn^{II} interact (anti-bonding) with filled porphyrin e_g orbitals below the valence orbitals, lowering the C-N breathing frequency. We note that there appears to be a general polarization effect on the ν_4 band, since Fe^{IV} heme, as exemplified by horseradish peroxidase compound II, shows an elevated frequency, 1382 cm^{-1} .³¹ On the other hand, Co^{II} vs. Co^{III} porphyrins show very small differences in this or any other frequency,^{32,33} as do Fe^{II} (low-spin) vs. Fe^{I} ³⁴ or Ni^{II} vs. Ni^{III}³⁵ tetraphenylporphyrins. In these cases the comparison is between low spin d^6 and d^7 , or d^7 and d^8 , configurations, which differ only in the occupancy of the d_{z^2} orbital; to first order this orbital does not interact with the porphyrin π orbitals.

C. Planar High-Spin Fe^{II} . When Fe^{II} porphyrin is coordinated by two weak field axial ligands, the result is in an in-plane structure in which the core is maximally expanded, owing to the antibonding interaction between the half-filled $d_{x^2-y^2}$ orbital and the pyrrole N atoms. This is exemplified by the structure of (THF)₂Fe^{II}TPP, whose core size (equal to the Fe-N (pyrrole) distance) is 2.057 Å,⁸ the largest observed in any Fe porphyrin. When the high-spin Fe^{II} heme is five-coordinate, the Fe moves out of the plane toward the fifth ligand, allowing the porphyrin core to relax, as in (2-MeImH)Fe^{II}TPP, with $C_{\text{I}}\text{-N} = 2.045$ Å (the Fe-N (pyrrole) bond length is actually increased, to 2.086 Å).²⁰

These structural parameters are of interest in connection with the mechanism of CO-heme photolysis, which involves very rapid (350 fs)³⁶ relaxation from the initially excited singlet $\pi\text{-}\pi^*$ state to a high-spin ligand field state,³⁷ which is dissociative with respect

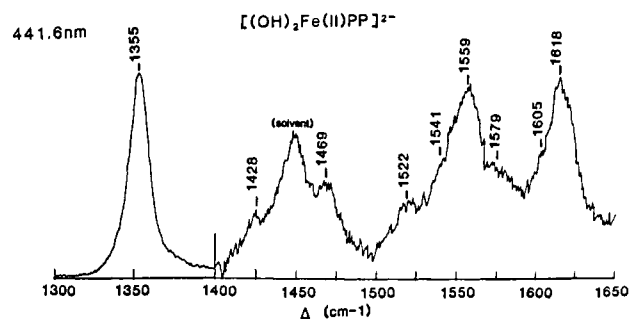


Figure 3. Raman spectrum of the complex $[(\text{OH})_2\text{Fe}^{\text{II}}\text{PP}]^{2-}$ prepared by adding sodium dithionite to hemin chloride in alkaline ethanol, according to the method of Keilin,⁹ with excitation at 441.6 nm near resonance with the B absorption band (452 nm).

to the CO. Consequently the rapidly formed high-spin six-coordinate Fe^{II} complex relaxes to a five-coordinate out-of-plane complex characteristic of deoxy heme. Since picosecond^{6a,b} and nanosecond^{6c,38} RR studies of the HbCO photoproduct showed small but reproducible frequency downshifts of porphyrin core-size marker bands, it was argued⁶ that the protein restrains the Fe atom from moving out of the plane for a significant period of time; the core-size marker frequencies were found to have relaxed by 300 ns.⁷ Indeed, a preliminary RR study of (THF)₂Fe^{II}OEP (OEP = octaethylporphyrin) suggested^{6b} that the photoproduct core-size frequencies were those expected of an in-plane high-spin Fe^{II} heme complex. It was subsequently recognized, however, that the core-size deviations for deoxy heme⁵ place its frequencies closer to those expected for a planar high-spin Fe^{II} heme, thus rendering the estimate of Fe out-of-plane displacement rather uncertain.

The Fe atom is unlikely to remain centered in the heme plane following CO dissociation owing to large uncompensated non-bonding forces between the proximal imidazole and pyrrole N atoms.³⁹ Molecular dynamic simulations of the CO dissociation⁴⁰ indicate that the out-of-plane displacement occurs on the femtosecond time scale. Indeed, a careful examination of the photoproduct core-size frequencies^{6c} show deviations from the core-size plots similar to those seen for deoxy heme, even when the comparison is made at 2.057 Å, the core size expected for the planar Fe^{II} high-spin heme. These deviations indicate that the porphyrin is domed in the photoproduct, because of the Fe out-of-plane displacement. Nevertheless, the shifts observed relative to deoxyHb do indicate a slightly expanded core, and it has been estimated^{6c} that protein forces restrain the out-of-plane displacement by ~ 0.1 Å, an amount not inconsistent with the molecular dynamic simulations.⁴⁰

It remains desirable to determine whether a planar high-spin Fe^{II} heme does in fact obey the core-size correlations (in the absence of porphyrin doming). We have examined $\text{Fe}^{\text{II}}\text{PP}$ in THF (solution) and found the results ambiguous, since the frequencies are quite close to those for (2-MeImH)Fe^{II}PP, and one cannot be sure that the bis-THF adduct is formed in solution; the only available titration data, in benzene solution, suggest a limiting five-coordinated species on addition of THF.⁴¹ We have tried to examine the RR spectrum of crystalline material obtained from the THF solution, on the assumption that it would be a bis-adduct like (THF)₂Fe^{II}TPP,⁸ but we found this material to be extraordinarily sensitive to laser irradiation, and the spectra were unreliable. We therefore turned to the species $[(\text{OH})_2\text{Fe}^{\text{II}}\text{PP}]^{2-}$, which can be prepared by addition of sodium dithionite to hemin chloride in alkaline alcoholic solution. Titration data leave no doubt that the bis-adduct is formed.⁹ Its B-band excited RR

(25) Yamamoto, T.; Palmer, G.; Gill, D.; Salmeen, I. T.; Rimai, L. *J. Biol. Chem.* **1973**, *248*, 5211.

(26) Spiro, T. G.; Streckas, T. C. *J. Am. Chem. Soc.* **1974**, *96*, 338.

(27) Kitagawa, T.; Iizuka, T.; Saito, M.; Kyogoku, Y. *Chem. Lett.* **1985**, *8*, 849.

(28) Spiro, T. G.; Burke, J. M. *J. Am. Chem. Soc.* **1976**, *98*, 5482.

(29) Shelnett, J. A.; Rousseau, D. L.; Friedman, J. M.; Simon, S. R. *Proc. Natl. Acad. Sci. U.S.A.* **1979**, *76*, 4409-4413.

(30) In a previously noted $C_{\text{I}}\text{-N}$ correlation for ν_4 , a negative deviation for the low-spin Fe^{III} representative was noted and attributed to porphyrin $\rightarrow \text{Fe}^{\text{III}}$ π donation, which might affect the primarily C-N stretching mode, but not the other modes.^{1b} The deviation is smaller (5 cm^{-1}) in the current correlation, based on more complete data, suggesting that the π -donation effect is not important.

(31) Rakhit, G.; Spiro, T. G.; Uyeda, M. *Biochim. Biophys. Res. Commun.* **1976**, *71*, 803.

(32) Woodruff, W. H.; Adams, D. H.; Spiro, T. G.; Yonetani, T. *J. Am. Chem. Soc.* **1975**, *97*, 1695-1698.

(33) Kim, D.; Miller, L.; Rakhit, G.; Spiro, T. G. *J. Phys. Chem.* **1986**, *90*, 3320.

(34) Strivatsava, G. S.; Sawyer, D. T.; Boldt, N. J.; Bocian, D. F. *Inorg. Chem.* **1985**, *24*, 2125.

(35) Kim, D.; Miller, L.; Spiro, T. G. *Inorg. Chem.* **1986**, *25*, 2468.

(36) Martin, J. L.; Nigus, A.; Poyant, C.; Lecarpentier, Y.; Astier, R.; Antonetti, A. *Proc. Natl. Acad. Sci. U.S.A.* **1983**, *80*, 173.

(37) Greene, B. I.; Hochstrasser, R. M.; Weisman, I. W.; Eaton, W. A. *Proc. Natl. Acad. Sci. U.S.A.* **1978**, *75*, 5255-5259.

(38) Lyons, K. B.; Friedman, J. M.; Fleury, P. A. *Nature (London)* **1978**, *275*, 2565.

(39) Friedman, J. M.; Rousseau, D. L.; Ondrias, M. R.; Stepnoski, R. A. *Science* **1982**, *218*, 1244.

(40) Henry, E. R.; Sommer, J. H.; Hofrichter, J.; Eaton, W. A. *J. Mol. Biol.* **1983**, *166*, 443.

(41) Brault, D.; Rougee, M. *Biochemistry* **1974**, *13*, 4591.

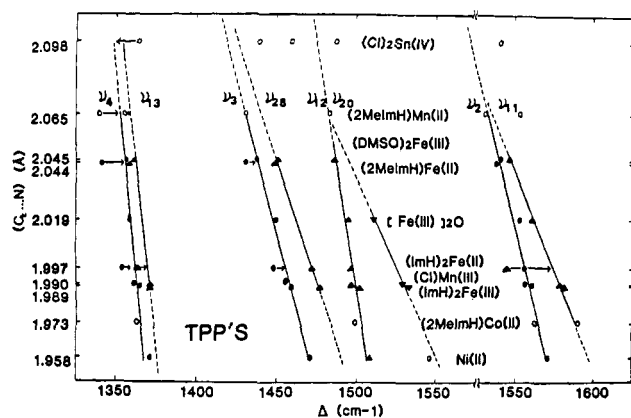


Figure 4. Core-size plot for TPP complexes (Table II). Symbols as for Figure 2.

spectrum is shown in Figure 3. It proved impossible to obtain Q-band-excited spectra owing to high backgrounds, possibly associated with fluorescent impurities. The frequencies associated with peaks identifiable as ν_4 , ν_3 , ν_2 , and ν_{10} are readily determined from the B-band spectrum, and shoulders can be seen which are probably associated with ν_{38} and ν_{37} . When these frequencies are placed on the core-size plots at $C_1-N = 2.057 \text{ \AA}$, the core size for the one structurally characterized high-spin bis-coordinate Fe^{II} porphyrin, $(\text{THF})_2\text{Fe}^{\text{II}}\text{TPP}$,⁸ they fall gratifyingly close to the best lines in every case (Figure 2). Thus, there seems little doubt that core-size relations do extend to planar high-spin Fe^{II} heme and can be used to estimate core-size changes following ligand dissociation, when the effects of five coordination (doming) are taken in account.^{6c} This conclusion strengthens the estimate from transient RR frequencies that the HbCO prompt photoproduct has a slightly larger heme core than deoxyHb, resulting from a $\sim 0.1\text{-\AA}$ restraint on the Fe out-of-plane displacement.^{6c}

D. TPP Core-Size Relations. Porphyrin structural chemistry is frequently studied via metal complexes of tetraphenylporphine, TPP, which is easy to synthesize and often yields diffraction-quality crystals more readily than physiological-type porphyrins. Although RR spectra of many metallo TPP's have been studied, the vibrational modes have only recently been catalogued and assigned.^{42,43} The different substituent patterns (phenyl groups on the methine C_m atoms and H on the pyrrole C_b atoms for TPP, but H on the methine C_m atoms and carbon substituents on the pyrrole C_b atoms for physiological-type porphyrins) lead to appreciable differences in the vibrational pattern. There is, nevertheless, a rough correspondence among the skeletal modes;^{1a} however, the mode numbering shifts down by one in the B_{1g} and A_{2g} blocks, because each contains an unobserved C-H stretching mode in TPP but not in PP.⁴²

Some time ago Stong et al.¹² noted that three of the high-frequency skeletal modes correlate with core size for a series of metallo TPP's (we note that the numbering systems used in ref 12 was later changed in ref 42), and Helms et al.⁴⁴ have recently used one of these correlations to probe the structural effect of electron-donating or -withdrawing substituents on the TPP phenyl rings and the resulting changes in exchange coupling for μ -oxo Fe^{III} dimers. Similar correlations have been noted by Blom et al.⁴⁵ for a series of metal complexes of tetrakis(4-*N*-methylpyridyl)porphine. We have examined RR spectra for the same series of TPP complexes as used for the PP core-size plot; the band frequencies and assignments are given in Table II, in which data are assembled for a large number of complexes investigated in this study or in the literature. Figure 4 shows that all of the

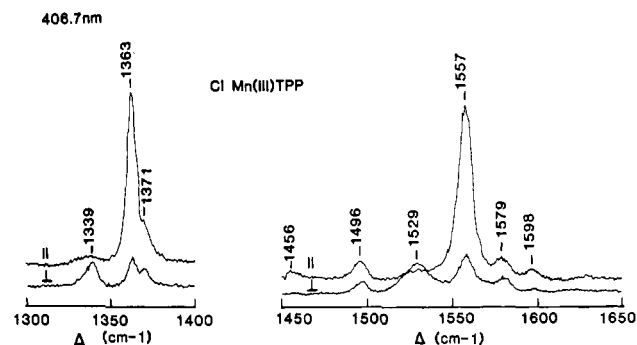


Figure 5. Raman spectra, in parallel and perpendicular polarization for $\text{ClMn}^{\text{III}}\text{TPP}$ in toluene with excitation at 406.7 nm near resonance with the higher component (397 nm) of the split B absorption band. Anomalous polarized bands corresponding to A_{2g} modes ν_{21} and ν_{20} are seen at 1339 and 1529 cm^{-1} .

high-frequency modes of TPP correlate with core size, just as they do for PP.

These data require a slight alteration of the mode assignments made in ref 42, because they reveal an additional depolarized mode in the $\sim 1450\text{-cm}^{-1}$ region, which was missed in the previous studies.^{42,43} It is weak, but appears consistently in different complexes, and it correlates with core size. Consequently we infer that it arises from a skeletal mode and assign it to the B_{2g} mode ν_{28} , involving C_a-C_b pyrrole bond stretching primarily. This mode had been assigned⁴² to a depolarized band found just above the strong polarized ν_4 , the A_{1g} C-N breathing mode. Since the core-size plot for this band runs parallel to ν_4 (Figure 4), we reassign it to ν_{13} (B_{1g}), which also involves symmetric (with respect to the pyrrole C_2 axis) stretching of the C-N bonds.⁴² This mode had been assigned to a depolarized band at 1271 cm^{-1} in $(\text{FeTPP})_2\text{O}$,⁴² which we now attribute to the previously unassigned ν_{29} (B_{2g}) mode, involving antisymmetric C-N stretching; it is expected at a frequency lower than the symmetric C-N modes.⁴² This set of reassignments, which is adopted in Table II and Figure 4, requires a minimum readjustment of the scheme worked out in ref 42.

Table III gives the slopes and intercepts of the linear correlations of Figures 2 and 4, according to the equation $\bar{\nu} = K(A - d) \text{ cm}^{-1}$, where $d = C_1-N$ (\AA). The modes for PP are listed in order of increasing core-size sensitivity, i.e., increasing K , and are compared with the corresponding TPP modes, taking into account that the TPP mode numbering slips by one for the B_{1g} and A_{2g} blocks. This listing emphasizes the relationship between the two quite different porphyrins. The values of the parameters are in the same range, and there is a rough parallelism in the order of increasing K , with ν_4 having the lowest value in each case. For ν_4 , ν_2 , and ν_{10} the values of K are actually quite similar, but for the remaining modes they differ substantially between PP and TPP. These differences no doubt reflect appreciable alterations in the normal mode compositions brought about by the differing substituent patterns.

The same complexes which deviate from the core-size plots for PP do so for TPP as well. Thus the points for the $\text{Cl}_2\text{Sn}^{\text{IV}}$ complex again fall well above the lines, reflecting the breakdown of the correlations for very large core sizes. $(\text{ImH})_2\text{Fe}^{\text{II}}\text{TPP}$ shows the expected back-bonding effect in a large frequency lowering of the B_{1g} mode ν_{11} , although the next B_{1g} mode, ν_{12} , does not show this effect. (The high-frequency deviations of the E_u modes seen in $(\text{ImH})_2\text{Fe}^{\text{II}}\text{PP}$ cannot be checked for TPP since these modes are not activated in the RR spectra.) The expected lowering of ν_4 is seen, as is a similar deviation for ν_{13} (a mode not seen in the PP complexes). Other ν_4 (and smaller ν_{13}) lowerings are seen for 2-MeImH complexes of Fe^{II} and $\text{Mn}^{\text{II}}\text{TPP}$, establishing the same oxidation state sensitivity for this mode as in PP (although in TPP the deviation for the high-spin Fe^{II} is actually greater than for the low-spin Fe^{II} complex). Thus the exceptions to the core-size correlations are qualitatively similar for PP and TPP.

E. Soret Enhancement of Anomously Polarized Modes in $\text{ClMn}^{\text{III}}\text{TPP}$. The RR spectrum of $\text{ClMn}^{\text{III}}\text{TPP}$ excited with 406.7 nm shows an interesting effect, namely resonance enhancement

(42) Stein, P.; Ullman, A.; Spiro, T. G. *J. Phys. Chem.* **1984**, *88*, 369-374.

(43) Burke, J. M.; Kincaid, J. R.; Spiro, T. G. *J. Am. Chem. Soc.* **1978**, *100*, 6077.

(44) Helms, J. G.; ter Haar, L. W.; Hatfield, W. W.; Harris, D. L.; Jayaraj, K.; Toney, G. E.; Gold A.; Mewborn, T. D.; Pemberton, J. R. *Inorg. Chem.* **1986**, *25*, 2334.

(45) Blom, N.; Odo, J.; Nakamoto, K.; Strommen, D. P. *J. Phys. Chem.* **1986**, *90*, 2847-2852.

of anomalously polarized (A_{2g}) bands at 1339 (ν_{21})⁴² and 1529 (ν_{20}) cm^{-1} , along with strong polarized bands at 1363 (ν_4) and 1557 (ν_2) cm^{-1} . The polarization spectra are displayed in Figure 5, and the stronger perpendicular scattering for ν_{21} and ν_{20} is clearly seen. Normally A_{2g} modes are seen only with Q-band excitation, enhancement being provided by their role in Q-B vibronic mixing. In principle equal enhancement should be seen in resonance with the B (Soret) band, via B-term scattering. Because of the large Soret absorption strength, however, A-term scattering, which enhances totally symmetric modes, is much stronger than B-term scattering,⁴⁶ and the A_{2g} modes are generally too weak to be detected. B_{1g} modes can frequently be seen with Soret excitation, because of their role in Jahn-Teller splitting of the doubly generate excited state.¹⁸

In the case of Mn^{III} porphyrins at least two strong absorption bands are seen in the Soret region giving a d-type hyperporphyrin spectrum, in Gouterman's classification.⁴⁷ The effect is attributed to a near-degeneracy of the Soret transition with a porphyrin $\pi \rightarrow \text{Mn } d_\pi$ charge-transfer transition. Being of the same symmetry (E_g) these transitions can mix and thereby share the absorption strength. For $\text{ClMn}^{\text{III}}\text{TPP}$, the split Soret bands are at 397 and 478 nm.⁴⁸ The 406.7-nm excitation wavelength is close to resonance with the higher energy of these two transitions. In an early study of $\text{ClMn}^{\text{III}}\text{TPP}$ Gaughan et al.⁴⁸ reported that with excitation at 488.0 nm, in resonance with the lower energy transition, the 1529- cm^{-1} peak (now known to be A_{2g}) is very weak in comparison to the other bands, most of which were depolarized.

The situation is similar to that reported recently by Terner and Topich¹⁴ for $(\text{NCS})(\text{MoO})\text{TPP}$, which also has a hyperporphyrin absorption spectrum. They found that excitation in the higher energy absorption enhanced polarized and anomalously polarized bands, while excitation in the lower energy absorption enhanced depolarized bands. For $\text{IMn}^{\text{III}}\text{TPP}$ the 1534- cm^{-1} anomalously polarized band was somewhat more strongly enhanced at 488 nm, although still less strongly than the depolarized bands.⁴⁸ It therefore appears that A_{2g} modes can be effective in mixing the two Soret-region transitions in metalloporphyrins with hyperporphyrin spectra. The symmetry for B-term scattering is the same as in the case of Q-B mixing:¹ the symmetries of the mixing

modes are contained in the direct product $E_g \times E_g = A_{1g} + A_{2g} + B_{1g} + B_{2g}$. The B_{1g} and B_{2g} , but not the A_{2g} modes, are also subject to A-term scattering via a Jahn-Teller distortion of the resonant state. It remains the case that B-term scattering should in general be weaker than A-term scattering because the latter scales with the square of the resonant state transition moment, while the former scales with the product of the resonant- and mixing-state moments, divided by the energy difference between the two states.⁴⁶ Nevertheless, the A_{2g} mode intensities in the Figure 5 spectrum are within an order of magnitude of the A_{1g} mode intensities, as is also the case in the 413.1-nm excited spectrum of $(\text{NCS})(\text{MoO})\text{TPP}$ reported by Terner and Topich.¹⁴ It appears that the A_{2g} modes are especially effective in mixing the two transitions. These modes transform as xy in the D_{4h} point group and have rotational symmetry. They mix the x component of the one transition with the y component of the other one. This rotational character may be especially effective in coupling the two transitions, which have varying amounts of charge transfer and $\pi-\pi^*$ character. It remains puzzling however, why the A_{2g} and B_{1g} , B_{2g} enhancements segregate as they do in the higher and lower energy transitions of $\text{ClMn}^{\text{III}}\text{TPP}$ and $(\text{NCS})(\text{MoO})\text{TPP}$.

Conclusions

The present work extends the previously noted core-size correlations of metallo PP skeletal modes to several complexes with transition metals other than Fe and Ni, and establishes their generality. Deviations are noted for certain classes of adducts, particularly low-spin Fe^{II} , and 2-MeImH adducts of several low-valent metals (Mn^{II} , Fe^{II} , and Co^{II}), reflecting superimposed electronic effects. The correlations break down for Sn^{IV} , probably reflecting a saturation of the core-size effect at very large core sizes. A core-size correlation is also discovered for the C-N breathing mode, ν_4 , but specific effects of oxidation state for Fe and Mn porphyrins are seen as negative deviations for the Fe^{II} and Mn^{II} species. The correlations are shown to hold well for the planar high-spin Fe^{II} heme, $[(\text{OH})_2\text{Fe}^{\text{II}}\text{PP}]^-$, lending confidence in the core-size analysis of the photoproduct RR spectra for HbCO. TPP derivatives are found to give core-size correlations corresponding to those of PP, but with altered slopes and intercepts, reflecting changes in the normal mode compositions due to the altered peripheral substituent pattern. An unusual instance of anomalous polarization is encountered for $\text{ClMn}^{\text{III}}\text{TPP}$, when excited in the higher energy of its two Soret absorption bands; this phenomenon may be general for metalloporphyrins with hyperporphyrin electronic spectra.

Acknowledgment. This work was supported by NIH Grant GM 33576.

Registry No. $(\text{Cl})_2\text{SnPP}$, 99022-74-9; (2-MeInH)MnPP, 108149-39-9; $[(\text{OH})_2\text{FePP}]^{2-}$, 108149-40-2; $[(\text{DMSO})_2\text{FePP}]^+$, 71860-79-2; (2-MeInH)FePP, 70085-59-5; $[(\text{Pip})_2\text{NiPP}]$, 108149-41-3; ZnPP, 15442-64-5; $[(\text{Cl})\text{FePP}]$, 16009-13-5; $(\text{InH})_2\text{FePP}$, 20861-23-8; $[(\text{Ac})\text{MnPP}]$, 108149-42-4; $[(\text{InH})_2\text{FePP}]^+$, 25875-11-0; (2-MeInH)CoPP, 108167-15-3; NiPP, 15415-30-2; $(\text{Cl})_2\text{SnTPP}$, 26334-85-0; (2-MeInH)MnTPP, 67180-30-7; $[(\text{DMSO})_2\text{FeTPP}]^+$, 68179-07-7; (2-MeInH)FeTPP, 48243-44-3; $[\text{FeTPP}]_2\text{O}$, 68136-95-8; $(\text{InH})_2\text{Fe}(\text{TPP})$, 19599-08-7; $\text{Mn}(\text{TPP})\text{Cl}$, 32195-55-4; $(\text{InH})_2\text{Fe}(\text{TPP})\text{Cl}$, 25442-52-8; (2-MeInH)-Co(TPP), 108149-43-5; NiTPP, 14172-92-0; (2-MeInH)CoPPDME, 64188-26-7.

(46) Tang, J.; Albrecht, A. C. In *Raman Spectroscopy Theory and Practice*; Szymanski, H. A., Ed.; Plenum Press: New York, 1970; Chapter 2, p 33.

(47) Gouterman, M. "Optical Spectra and Electronic Structure of Porphyrins and Related Rings" In *The Porphyrins*; Dolphin, D., Ed.; Academic Press: New York, 1978; Vol. III, p 1.

(48) Gaughan, R. R.; Shriver, D. F.; Boucher, L. J. *Proc. Natl. Acad. Sci. U.S.A.* **1975**, *72*, 433.

(49) Gonzalez, B.; Kouba, J.; Yee, S.; Reed, C. A.; Kirner, J. F.; Scheidt, W. R. *J. Am. Chem. Soc.* **1975**, *97*, 3247.

(50) Mashiko, T.; Kastner, M. E.; Spartalian, K.; Scheidt, W. R.; Reed, C. A. *J. Am. Chem. Soc.* **1978**, *100*, 6354.

(51) Kirner, J. F.; Garofollow, J., Jr.; Scheidt, W. R. *Inorg. Nucl. Chem. Lett.* **1975**, *11*, 107.

(52) Scheidt, W. R.; Kastner, M. E.; Hatano, K. *Inorg. Chem.* **1978**, *17*, 706.

(53) Hoard, J. L. *Science* **1971**, *174*, 295.

(54) Radonovich, L. J.; Bloom, A.; Hoard, J. L. *J. Am. Chem. Soc.* **1972**, *94*, 2073.

(55) Collins, D. M.; Countryman, R.; Hoard, J. L. *J. Am. Chem. Soc.* **1972**, *94*, 2066.

(56) Scheidt, W. R. *J. Am. Chem. Soc.* **1974**, *96*, 90.